

RESEARCH ARTICLE

Uncoiling springs promote mechanical functionality of spider cribellate silk

Dakota Piorkowski¹, Todd A. Blackledge², Chen-Pan Liao^{1,3}, Anna-Christin Joel⁴, Margret Weissbach⁴, Chung-Lin Wu⁵ and I.-Min Tso^{1,6,*}

ABSTRACT

Composites, both natural and synthetic, achieve novel functionality by combining two or more constituent materials. For example, the earliest adhesive silk in spider webs – cribellate silk – is composed of stiff axial fibers and coiled fibers surrounded by hundreds of sticky cribellate nanofibrils. Yet, little is known of how fiber types interact to enable capture of insect prey with cribellate silk. To understand the roles of each constituent fiber during prey capture, we compared the tensile performance of native-state and manipulated threads produced by the cribellate spider *Psecrus clavus*, and the adhesion of native threads along a smooth surface and hairy bee thorax. We found that the coiled fiber increases the work to fracture of the entire cribellate thread by up to 20-fold. We also found that the axial fiber breaks multiple times during deformation, an unexpected observation that indicates: (i) the axial fiber continues to contribute work even after breakage, and (ii) the cribellate nanofibrils may perform a previously unidentified role as a binder material that distributes forces throughout the thread. Work of adhesion increased on surfaces with more surface structures (hairy bee thorax) corresponding to increased deformation of the coiled fiber. Together, our observations highlight how the synergistic interactions among the constituents of this natural composite adhesive enhance functionality. These highly extensible threads may serve to expose additional cribellate nanofibrils to form attachment points with prey substrata while also immobilizing prey as they sink into the web due to gravity.

KEY WORDS: Biofiber, Spider web, Adhesion, *Psecrus clavus*, Composite material

INTRODUCTION

Composite materials combine individual constituents into a new material with characteristics that are different from the starting materials (Elhajjar et al., 2013; Jones, 2014). Concrete, papier-mâché and fiber-reinforced plastics are common examples of synthetic composite materials (Cantwell and Morton, 1991; Jones, 2014), while seashells, hair and spider silk are notable examples in nature (Mayer and Sarikaya, 2002; Popescu and Höcker, 2007;

Blackledge and Hayashi, 2006a). Typically, reinforcing materials with unique properties are embedded within a matrix material that support the reinforcers, such as pieces of paper in water in papier-mâché or the hard layers of a mollusk shell supported by softer layers (Mayer and Sarikaya, 2002; Jones, 2014). Spider capture silks are composed of a strong core fiber supporting sticky, highly pliable glue (viscid) or nanofibrils (cribellate). The combination of these materials produces composite adhesives that use strength and extensibility of constituent silks to retain struggling insect prey caught in spider webs (Hawthorn and Opell, 2003; Opell and Hendricks, 2007; Sahni et al., 2010). Here, we describe the mechanical contributions of components of a previously uncharacterized type of cribellate thread that includes an additional silk fiber with a coiled morphology.


Cribellate silk is the earliest known adhesive capture thread to evolve in spiders and is still used within webs by up to 22 ecologically diverse families of spiders (Griswold et al., 1999). Across families, this composite thread demonstrates considerable variability in the number and type of silk fibers with at least three unique fiber types (Eberhard and Pereira, 1993; Griswold et al., 2005). Generally, cribellate silk threads share two common features: cribellate nanofibrils produced from the plate-like cribellum that are combed out by the calamistrum on the spider's hindlegs and a pair of axial silk fibers produced in the pseudoflagelliform glands (Eberhard and Pereira, 1993; Kovoov, 1987; Joel et al., 2015). Cribellate silk attains 'stickiness' via the cribellate nanofibrils through a combination of van der Waals and hygroscopic forces along with physical interaction with microscopic surface features, such as hairs on an insect cuticle (Eberhard, 1988; Hawthorn and Opell, 2003; Bott et al., 2017). These adhesive properties have also been speculated to help bind the other constituent silks together (Eberhard and Pereira, 1993). Paracribellate fibrils, produced by the paracribellum in at least 13 families (Griswold et al., 2005), form a bundled substructure that is also hypothesized to conjoin the cribellate nanofibril mass to the axial fibers (Peters, 1984; Joel et al., 2015). Axial fibers of cribellate threads are stiff and strong, and provide support for the cribellate nanofibrils (Blackledge and Hayashi, 2006a). Twenty-one families of cribellate spider include an additional type of silk fiber with a morphology similar to a coiled spring, variously known as the reserve warp, undulating fiber or coiled fiber, as we will refer to this silk fiber hereafter (Eberhard and Pereira, 1993; Griswold et al., 2005). Previous observations of coiled silk from *Kukulcania hibernalis* report that these fibers unfolded as the cribellate thread is extended and are extruded from minor ampullate spigots (Eberhard and Pereira, 1993; Grannemann et al., 2019).

The geometry of a coiled spring engages shear stresses (torsional forces) rather than tensile stresses during initial axial deformation. This allows even very stiff materials, e.g. hardened steel, to improve axial deformation and compliance, as shear modulus of a given

¹Department of Life Science, Tunghai University, Taichung 40704, Taiwan.

²Department of Biology, Integrated Bioscience Program, The University of Akron, Akron, OH 44325, USA. ³Department of Biology, National Museum of Natural Science, Taichung 40453, Taiwan. ⁴Institute of Biology II, RWTH Aachen University, 52074 Aachen, Germany. ⁵Center for Measurement Standards, Industrial Technology Research Institute, Hsinchu 30011, Taiwan. ⁶Center for Tropical Ecology and Biodiversity, Tunghai University, Taichung 40704, Taiwan.

*Author for correspondence (spider@thu.edu.tw)

 D.P., 0000-0003-1405-1020; T.A.B., 0000-0002-8166-5981; C.-P.L., 0000-0001-9703-1994; A.-C.J., 0000-0002-7122-3047; I.-M.T., 0000-0002-7296-5595

material tends to be lower than elastic modulus (Ashby and Cebon, 1993). Spring-like structures, such as metal-alloy coiled springs in trampolines and clocks or vertebrate tendons and mantis shrimp heels in animals, are typically designed to store and release kinetic energy within an elastic limit (Ashby and Cebon, 1993; Patek et al., 2004; Roberts and Azizi, 2011). However, for silk in spider webs, dissipation of energy is far more important to prey capture than the release of energy, which may ricochet an insect out of the web (Blackledge et al., 2011). For instance, recluse spiders increase the mechanical toughness of the flattened silk threads incorporated into their webs by producing loops with sacrificial bonds (Koebley et al., 2017). Coiling of silk may be another way in which spiders can improve the overall work of a composite capture silk by increasing extensibility, via more silk per length, and by incorporating shear forces along with tensile forces.

Earlier work by Blackledge and Hayashi (2006a) showed that cribellate silk produced by uloborid orb web spiders extended less than 100% its length, remarkably less than the better characterized viscid capture threads in late diverging orb spiders. Most of the work to deform these cribellate threads came from the axial fibers, which stretched 2–3 times less than the nanofibrils, but generated 3–5 times as much force. However, uloborid cribellate silk lacks coiled fibers and contains axial fibers with paracribellate fibers and cribellate nanofibrils. Blackledge and Hayashi (2006a) also tested cribellate silk of the ogre-faced deinopid spider *Deinopis spinosa* and found extensibility up to ~500% of its original length. Moreover, load continued to increase by nearly 100% after the axial fiber broke. Blackledge and Hayashi (2006a) also identified a ‘coiled thread’, which has also been identified in other *Deinopis* species (Kullmann, 1975; Peters, 1992b), which they hypothesized may have contributed to this extra work but did not explicitly characterize its performance. Cribellate capture silk of the odd-clawed gradungulid spider *Progradungula otwayensis* also contains a coiled fiber and was shown to extend to 1400% its original length, making it one of the most extensible spider threads known (Michalik et al., 2019). This was largely ascribed to structural changes in the thread morphology during extension (Michalik et al., 2019); however, explicit testing of individual contributions of fibers during performance has not been done.

Viscid silk is another kind of adhesive composite silk used in spider orb webs to capture prey (Foelix, 2011). Cribellate silk predates the emergence of ecribellate silk (Blackledge et al., 2009; Garrison et al., 2016) and, aside from functional similarities in prey capture, is very dissimilar in morphology, production and mechanical performance (Köhler and Vollrath, 1995; Piorkowski and Blackledge, 2017). The underlying flagelliform fiber is coated in an aqueous glue, rather than nanofibrils, that is more quickly drawn out by the spider (Zschokke and Vollrath, 1995). Water content of the glue plasticizes the flagelliform fiber, allowing the threads to extend 100–300% (Gosline et al., 1984; Vollrath and Edmonds, 1989; Swanson et al., 2007). This synergistic interaction gives rise to the suspension bridge mechanism, a process by which up to 50% of adhesive work is transferred from glue to the silk fiber (Opell and Hendricks, 2007; Sahni et al., 2010). The high compliance and extensibility of the thread allows efficient absorption of kinetic energy from the movement of prey caught in webs and helps prevent permanent damage or breakage of the threads (Opell and Schwend, 2009). We hypothesize that forces may be similarly transferred to the coiled fiber in cribellate threads during prey capture.

To determine the mechanical contribution and possible role in prey capture of coiled fibers in cribellate silk, we performed tensile and adhesive tests on threads produced by the lace-sheet spider

Psechrus clavis (Araneae: Psechridae, Bayer, 2012; Fig. 1A). This species is a large nocturnal spider native to Taiwan that builds horizontally oriented sheet webs and also uses its cribellate silk as a prey lure (Lai et al., 2017; Fig. 1B). Compared with other cribellate species, *P. clavis* (along with other members of *Psechrus*) produces a relatively simple cribellate silk morphology. Each cribellate silk thread is composed of one axial fiber and one coiled fiber, surrounded by a matted cribellate nanofibril shroud (Fig. 1C). Because of the simple thread structure, silk from this species is an ideal model for disentangling the mechanical contributions of each fiber type, particularly the mostly unknown coiled fiber, within the cribellate silk composite. For tensile tests, threads were tested in their native state or were manipulated with either the axial or coiled fiber cut at one end. During early testing, we made the unexpected discovery that axial fibers can break more than once; therefore, we provide additional visual and mechanical evidence to support this observation. Finally, we tested adhesive properties of these cribellate threads when in contact with different surface types (smooth synthetic surfaces versus hairy insect cuticle).

MATERIALS AND METHODS

Our methods for silk collection, tensile testing and adhesion testing are similar to those previously used by Piorkowski and Blackledge (2017) and Piorkowski et al. (2018a), with the modifications noted below.

Silk collection and manipulation

We collected 315 cm² sections from webs of 29 *P. clavis* sub-adult females inhabiting a trail within forest surrounding the Low-Altitude Research Station, Taiwan Endemic Species Research Institute (TESRI), Wu-Shi-Keng, Taichung city, Taiwan (120°60'

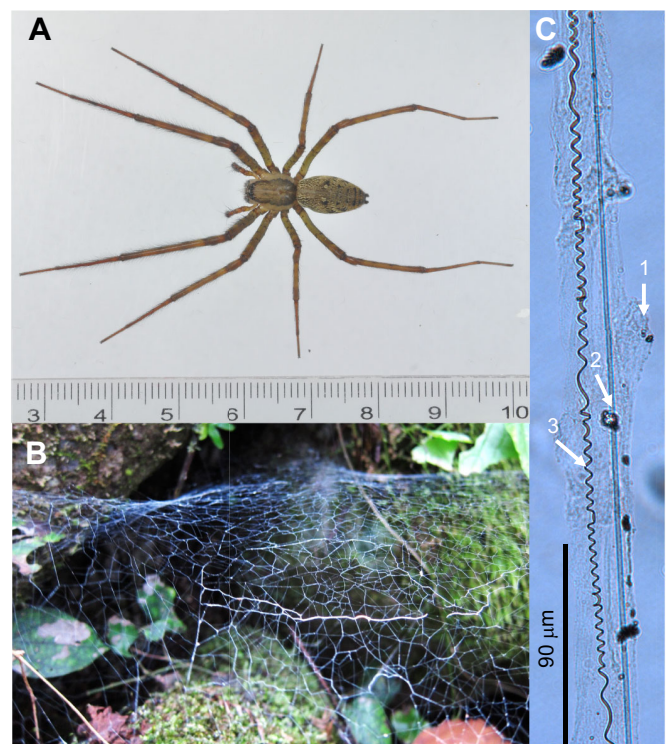


Fig. 1. *Psechrus clavis* adult, web structure and cribellate silk thread. (A) An adult female (scale: cm) and (B) a freshly constructed web with blue cribellate threads prominent. (C) Cribellate capture silk with numbers indicating the constituents of a thread: (1) cribellate nanofibrils, (2) axial fiber and (3) coiled fiber.

22.45°E, 24°17′0.86″N) in January 2015 and February 2019. Webs of this species are occupied by a single resident spider (Lai et al., 2017); therefore, we only collected from inhabited webs without significant damage. The most accessible fresh cribellate silk (identified by a blue color, Fig. 1B) near the edge of the web or within it was sampled. Samples were attached to circular wooden frames (diameter: 20 cm) affixed with double-sided sticky tape, to maintain the original tension of the web and ensure preservation of the web samples.

Sections of sampled webs were transported within 3 h from the field to the laboratory at Tunghai University, Taiwan. Cribellate silk threads and frame threads composed of major ampullate silk are irregularly interspersed throughout the web (see Fig. 1B) and regularly intersect with cribellate silk threads. We sub-sampled 5–8 undamaged cribellate silk threads (15 mm in length) with minimal to no visual display of dust or debris. Cribellate silk threads were extracted from webs and suspended across U-shaped collecting frames with 10 mm wide gaps cut out of one end of 26 mm×15 mm cardboard cards. On rare occasion (<5% of silk samples used), small fragments (1–2 mm) of web frame threads remained in contact with collected cribellate threads. This was an artifact of sampling as non-overlapped 15 mm segments of cribellate silk threads were not always accessible. We did not notice any significant effect of the presence of these fragments of frame silk threads. Cribellate threads were initially affixed to frames by exploiting their natural adhesiveness and later reinforced with Elmer's glue.

Prior to tensile testing, we manipulated 21 total threads by cutting either the axial fiber ($N=10$ individuals, $n=11$ threads; see Fig. S1) or the coiled fiber ($N=10$, $n=10$; see Fig. S2) at one end of the fiber near the edge of the cardboard frame. We used a thin steel wire (diameter: 15 μm) affixed to a bamboo chopstick with tape to carefully pull silk fibers away from cribellate nanofibrils and the other intact silk. Once a silk fiber had been successfully pulled away from the bundle of fibers, the fiber was cut using small dissection scissors. Damage to the cribellate nanofibrils is to be expected as they adhere to both the steel wire and scissors and completely enclose the other silk fibers. Samples where both silk fibers (axial and coiled) and/or large amounts of cribellate nanofibrils were visually damaged were not used for testing.

Scanning electron microscopy of spinnerets

Imaging of *P. clavis* spinneret morphology was conducted using spiders collected in Taiwan from the same study site and preserved in 70% ethanol before being sent to Aachen University, Germany. Samples must be dried for successful sputter coating. Therefore, an ascending ethanol concentration series was used to remove all water content, then the sample was further dried overnight in hexamethyldisilazane. This chemical evaporates very quickly but reacts to water, hence the requirement for prior ethanol exposure. Specimens were then sputter coated with a ~10 nm layer of gold (Hummer Technics Inc.) before examination using a scanning electron microscope (SEM 525 M; Philips AG, Amsterdam, The Netherlands).

Tensile testing

The tensile properties of 48 cribellate threads sampled from 25 individual *P. clavis* webs were determined within 2 weeks of collection, using two similar Nano Bionix[®] tensile testers (MTS Systems Corp., Eden Prairie, MN, USA) at the University of Akron in February 2015 and the Industrial Technology Research Institute in Hsinchu in March, 2019. Testing conditions in the two facilities

were similar (~45% relative humidity, ~20°C). A previous study by Piorkowski et al. (2018a) showed that data collected from the two machines showed similar tensile performance for glowworm silk, which we also found for silk tested in this study. Therefore, we combined datasets collected for measurements on the two machines.

To determine the tensile properties of cribellate silk of *P. clavis*, threads (10 mm gauge length) were mounted vertically between the upper and lower grips of the machine. Load–extension data were generated for each cribellate thread collected by pulling them to rupture at an extension rate of 1.5% s^{-1} in the tensile tester (Blackledge and Hayashi, 2006a). Threads did not always completely break at the peak force registered during a test, so we determined overall peak force of the composite thread and percentage extension at break (calculated as total thread extension/gauge length×100). We calculated work to break as total area under the load–extension curve.

Given the multiple silk types involved in this thread composite, i.e. coiled fiber, axial fiber and cribellate nanofibrils, and the structural complexity of this system, i.e. unaligned and slack morphology of the nanofibrils and coiled fiber along with the taut axial fibers, we did not calculate stress and strain like most other studies on spider silk. These measures are useful as they have built-in normalization that accounts for differences in silk dimensions which helps to control for variation between spiders but they are specifically designed to allow comparison of discrete materials rather than composite structures. We measured axial fiber diameter of 10 individuals using polarized light microscopy (Blackledge et al., 2005), with accuracy to 0.1 μm , to establish variation in body size and found that all diameters fell within a relatively small range of 0.9–1.4 μm . Therefore, we assume that differences in silk diameter and structural attributes between individual spiders do not strongly influence our results as these are very minor compared with the differences among the different fiber types in these threads. Finally, our experiment was designed to be as pairwise as possible, focusing on differences between treatments within silk from the same individual spider (see ‘Statistical analysis’, below).

Visual characterization of silk fiber breakage

Additional investigation was conducted to determine the source of the unusual drops in load that occurred during tensile testing and observe changes in thread morphology. Eight samples in total were observed at 40% extension, the first and second major drops in load (defined as a decrease in $\geq 50\%$ load over $\leq 5\%$ extension), and at $>250\%$ extension. Tensile tests were paused and samples were carefully unmounted from the tensile tester using clamps to maintain thread tension. Samples were then transferred to a polarized light microscope (Leica DMLB, Meyer Instruments) and scanned at 10× magnification across their entire length. Samples were remounted for further stretching and observation.

To examine axial fiber breaks using scanning electron microscopy, thread samples were fixed between a micromanipulator and the microscope stage of a VW-9000 high-speed microscope (Keyence Cooperation). Samples were then slowly and manually stretched longitudinally, by pulling either the microscope stage or the micromanipulator, while observing a section of sample at $>100\times$ magnification. Before complete rupture of the entire thread, samples were affixed to an scanning electron microscope sample holder. Images of areas of axial breaks were taken via scanning electron microscopy (acceleration voltage: 15 kV, spot size: ~40 nm) without any previous treatment or coating of the sample. As shown in Joel and Baumgartner (2017), uncoated cribellate thread samples do not show any effects from charging during imaging.

Adhesion testing

The adhesive properties of 38 cribellate threads sampled from 13 individual *P. clavis* webs were determined using the abovementioned facilities. As with the aforementioned tensile testing, and similar to a previous study by Piorkowski et al. (2018a), data collected from the two machines showed similar adhesive performance for capture silk. Therefore, we combined datasets collected for measurements on the two machines.

We used a smooth synthetic surface (2 mm×5 mm fragment, standard silicon wafer of 10.16 cm radius, 525 μm thickness) and the thorax of intact bodies of hairy bees (5 mm×5 mm, *Apis mellifera*, collected from local farms in Akron, OH, USA, 12 months prior to testing) to test the adhesive properties of cribellate silk of *P. clavis* (see Fig. 2 for set-up). Prior to testing, silicon wafer fragments were mounted onto brass supports and hairy bee bodies were mounted on the tips of steel pins (1 mm diameter) using cyanoacrylate glue. Hairy bee bodies were mounted on the lower grips of the tensile tester with their dorsal side facing up using clay putty to affix the supporting pin. The silicon wafer fragment was positioned horizontally as the brass mount was clamped between the lower grips of the tensile tester. Cribellate threads (gauge length 10 mm) were mounted horizontally as collecting frames were clamped between the upper grips of the extension arm of the tensile tester. The thread was lowered onto the substrate with a force of 15 μN applied for 20 s, thus ensuring firm and direct contact. The thread was then pulled off the stage at a rate of 0.1 mm s⁻¹. Load–displacement curves were generated as the thread detached from the substrate and work of adhesion was calculated as the area under these curves. Adhesion in uloborid

cribellate threads is generated at the edges of contact, as opposed to along the entire length of contact as in viscid silk threads, and substrate width in contact with the thread is not correlated with adhesive force generated (Opell and Schwend, 2009). Therefore, we did not normalize force by substrate width. However, given that substrate dimensions were not equal between treatments, extension was normalized by length of fiber not in contact with the substrate. Work of adhesion was not normalized, as all samples were equal in total gauge length. Additionally, silicon wafer surfaces were cleaned with isopropyl alcohol after every test. Each thread sample was tested once (silicon wafer: $N=9$ individuals, $n=15$ samples, bee thorax: $N=3$, $n=7$).

Additional tests were conducted with a bee thorax as the substrate ($N=2$, $n=2$) that were modified in the following ways: the silk sample was mounted vertically rather than horizontally; the bee was tilted at 45 deg from horizontal rather than being fully upright; samples were shifted laterally into the surface until apparent contact was made; and the lower frame edge below the thorax was cut away from the frame to avoid interference from the frame itself during testing (see Fig. S3 for set-up).

Statistical analysis

We fitted tensile properties and adhesive properties in two independent multivariate general linear mixed-effect models by using the R package ‘brms’ (version 2.7.0; Bürkner, 2017). Thread type, reflecting manipulations to constituent fibers, and surface type were included as a fixed factor to compare the tensile and adhesive properties, respectively. Spider identity and a fixed factor within each spider individual were both included as correlated random intercepts to control for pseudoreplication. All independent variables were natural-log transformed before model fitting. We assigned weakly informative priors for all parameters (i.e. intercept term, 10 times scaled t distribution with d.f.=3; fixed effect, 5 times scaled t distribution with d.f.=7; standard deviations of random effect and residual, 5 times scaled positive t distribution with d.f.=3). Ten-thousand Markov chain Monte Carlo (MCMC) iterations (including the beginning 8000 burn-in iterations) per thread were performed, and in total tests for 10 threads were performed in parallel for each parameter. Pair-wise Bayesian MCMC equivalence tests in each dependent variable were conducted, and we assigned the region of practical equivalence (ROPE) as 0.8–1.25. Only the posterior distribution of the ratio of a specific property between two levels of the fixed factor completely lying outside the ROPE was considered as significant.

RESULTS

Cribellate thread production

The primary constituents of *P. clavis* cribellate silk threads are produced from spigots of the posterior and median spinnerets, as well as the cribellum (Fig. 3A,B). The axial fiber is presumably extruded from the spigots of the pseudoflagelliform gland, one on each posterior spinneret (Fig. 3C), as described for other species (Peters, 1984, 1992b; Joel et al., 2015). The coiled fiber is described as being extracted from the minor ampullate gland spigot of the median spinnerets (Peters, 1992a,b; Grannemann et al., 2019), which is also present in *Psechrus* spiders (Fig. 3D). The cribellate nanofibrils are organized as a mat, without any secondary hierarchical structure, like the puffs seen in many other species (Fig. 1C), and are extruded by the cribellum (Fig. 3E). *Psechrus* spiders possess a divided cribellum (Griswold et al., 2005, Fig. 3E) and, therefore, always produce two parallel capture threads. Each thread consists of one axial fiber and one coiled fiber, not visibly connected to each

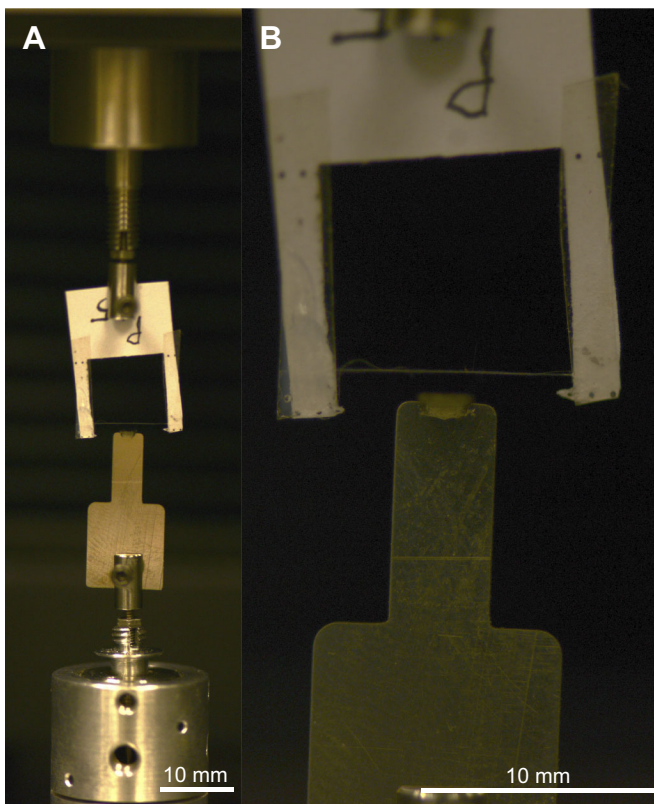


Fig. 2. Adhesion testing set-up. (A) Overview and (B) close-up image of the apparatus. Cribellate silk threads were pressed into and pulled off silicon wafer surfaces. Gauge length of the cribellate silk thread is 10 mm and width of the silicon wafer fragment width is 2 mm.

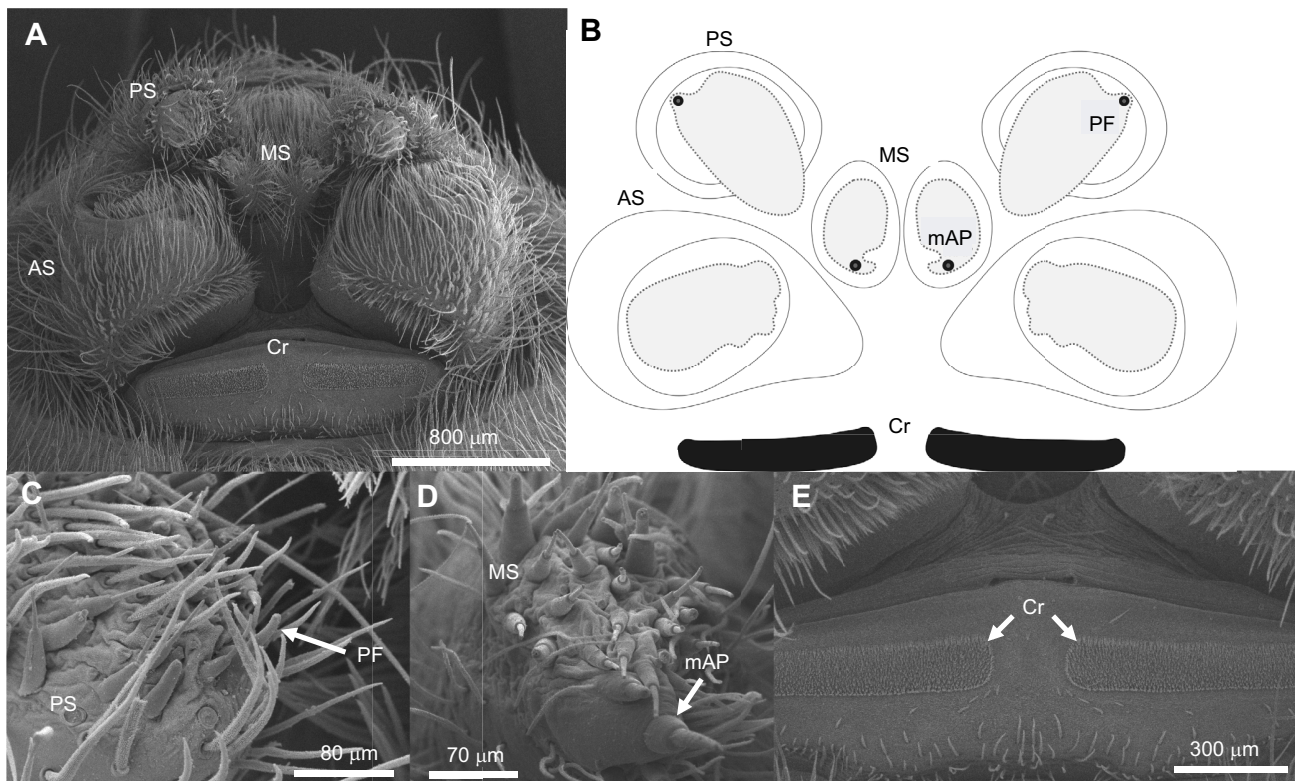


Fig. 3. *Psechrus clavus* spinneret morphology. (A) Ventral view and (B) diagram of *P. clavus* anterior (AS), median (MS) and posterior (PS) spinnerets and divided cribellum (Cr) with location (B) and close-up views (C–E) of the pseudoflagelliform spigots (PF, source of axial fiber), minor ampullate spigot (mAP, putative source of coiled fiber) and divided cribellum (Cr). Images were taken from the same sub-adult female.

other (Fig. 1C). Based on online video recordings of *Psechrus mulu* (see https://www.youtube.com/watch?v=02RZe0c_VHo, <https://www.youtube.com/watch?v=gwG2-YG4KXc>; both accessed on 20 May 2019), which also possesses a divided cribellum (Griswold et al., 2005), we observed the two cribellate threads are separated during production by attaching each thread in parallel to, but separated from, the radial lines of the web. *Psechrus* spiders do not possess paracribellate spigots (Griswold et al., 2005) and, accordingly, paracribellate fibers were not found in the thread, nor was a paracribellum identified (Figs 1C and 3A). No connection, such as knotting or additional silk, was detected between any of the three fiber types.

Tensile performance

Native-state threads demonstrate an initial elastic region followed by a yield point, where the slope of the force–extension curve changes, followed by gradually increasing force with extension, similar to cribellate silk of other species and other silk types (Blackledge and Hayashi, 2006a,b). After 35–120% extension, we observed a sharp drop in force (Fig. 4A), which was verified to be the first break of the axial fiber using light microscopy (Fig. 4B) and scanning electron microscopy (Fig. 4C). After this point, force–extension curves began to demonstrate minor fluctuations in force (± 0.01 mN) with a gradual recovery in force over 20–60% extension (Fig. 4A) that is likely ascribable to unraveling and breaking of unaligned cribellate nanofibrils and uncoiling of the coiled fiber. As force values reached or slightly surpassed that of the initial axial fiber break, a second drop in force was observed (Fig. 4A). We verified that the axial fiber can break at least twice (Fig. 4B; Movie 1), and observed a maximum of five breaks. The axial fiber may continue to break

throughout extension, as we observed force drops and recovery throughout extension. However, we were unable to visually verify additional breaks at extensions beyond 200–250%. Around this point, the coiled fiber becomes fully taut and lateral distance to the axial fiber decreases until these fibers are nearly touching, severely obstructing visualization of the axial fiber. The point at which the coiled fiber fully uncoils and begins axial elongation is reflected in the force–extension curve as a gradual increase in loading and change in slope (Fig. 4A, point 5). Typically, failure of the coiled fiber coincided with failure of the entire composite, confirmed by both tensile data and visual observation. However, there were seven instances out of 27 tests of the coiled fiber failing just before the whole thread (see Fig. 4A). The final extension of the thread is presumably ascribable to the remaining, unbroken cribellate nanofibrils, although the load generated is very low by comparison (<0.05 mN).

Compared with native-state threads, threads with a cut coiled fiber achieved 5 times less extension at break, 4 times lower peak force and performed an order of magnitude less work at break (Fig. 5A–C, Table 1). Manipulated coiled fibers were not engaged during extension and threads typically failed at the first axial fiber break, although we did observe 3 instances of multiple axial breaks out of 10 tests. Threads with cut axial fibers were not significantly different in performance to native-state threads (Fig. 5A–C, Table 1). However, these threads were qualitatively less stiff than native threads during extension (Fig. 5D).

Adhesive performance

Extension at detachment (mean \pm s.d., bee thorax: 1.092 ± 0.672 mm, smooth surface: 0.141 ± 0.096 mm) and work of adhesion (bee

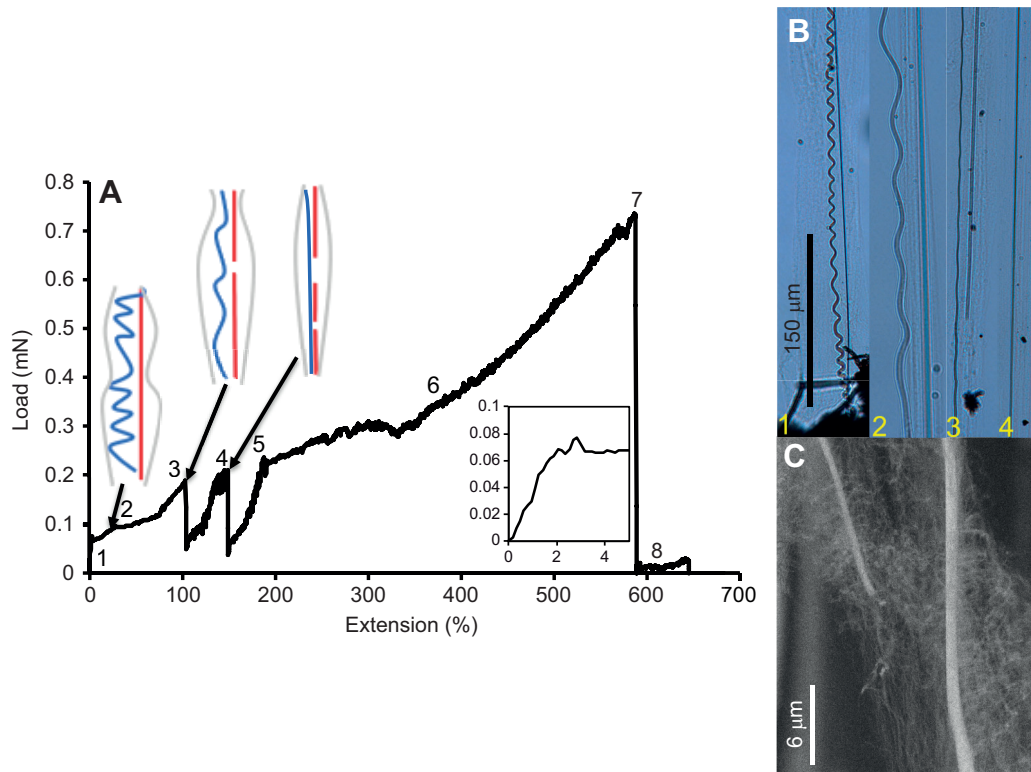


Fig. 4. Mechanical behavior of *P. clavus* cribellate threads. (A) Representative load–extension curve of a 10 mm cribellate silk thread from a *P. clavus* web pulled to breaking at $1.5\% \text{ s}^{-1}$. Blue, coiled thread; red, axial fiber. Inset, initial stiffness of cribellate thread. (B) Corresponding changes in morphology and (C) close-up of cribellate thread post-axial breakage. Numbers indicate important events during stretching: (1) region of initial stiffness of the thread followed by a yield point, (2) post-yield change in slope and extension, (3) first break of the axial fiber, (4) second break of the axial fiber, (5) the coiled fiber is fully uncoiled and begins axial elongation, (6) the majority of constituent silks are tensed and deforming, (7) coiled fiber failure (typically when the entire thread fails $n=20$ of 27 total tests), (8) in some cases ($n=7$) the cribellate nanofibrils continue to deform.

thorax: $0.251 \pm 0.249 \mu\text{J}$, smooth surface: $0.010 \pm 0.015 \mu\text{J}$) generated by cribellate threads were significantly greater in tests conducted on bee thorax substrates than those on smooth silicon wafer surfaces (Fig. 6A,C, Table 2). Force of detachment (bee thorax: $0.056 \pm 0.035 \text{ mN}$, smooth surface: $0.012 \pm 0.011 \text{ mN}$) was not significantly different between the two substrates (Fig. 6B; Table 2). These values are comparable to those reported from tests using smooth surfaces for *Hypochilus* and *Hyptiotes* cribellate spiders (0.015 – 0.055 mN ; Hawthorn and Opell, 2003), but are lower than those reported for *Uloborus* and *Octonoba* species (0.07 – 0.13 mN ; Opell and Schwend, 2009) and much lower than those from tests on insect cuticle ($\sim 0.25 \text{ mN}$; Bott et al., 2017). The coiled and axial fibers deformed considerably during adhesion to the bee thorax (Fig. 6D; Movie 2) and remained intact after detachment. The morphology of

the coiled fiber was permanently altered at and near the point of attachment as the fiber partially uncoiled and did not completely return to its original form.

Two additional tests were conducted, which are not included in our formal statistical analysis, where a bee body was tilted 45° from vertical and one side of the collecting frame was detached to allow vertically oriented threads to freely stretch while still in contact with the bee thorax (Fig. S3). During these tests, we observed breakage of the axial fiber, along with uncoiling and stretching of the coiled fiber. Peak force values (0.1 mN mm^{-1}) were close to what has been observed previously for adhesion of cribellate silk to insect cuticles (Bott et al., 2017). Additionally, these threads stretched 261 – 359% before detachment, which is more than half of the extensibility of the overall thread ($\sim 500\%$).

Table 1. Results of multiple comparisons of tensile properties among each thread type

Dependent variable	Comparison	Difference	Ratio
Extension at detachment (%)	Coil cut vs native state	−40.24 (−53.18, −28.05)	0.2078 (0.1313, 0.3301)
	Coil cut vs axial cut	−29.59 (−46.03, −14.24)	0.2659 (0.1514, 0.4604)
	Native state vs axial cut	10.66 (−9.079, 30.22)	1.1543 (0.8088, 1.5218)
Peak force (mN)	Coil cut vs native state	−0.7051 (−0.9243, −0.5651)	0.2575 (0.1897, 0.3583)
	Coil cut vs axial cut	−0.6310 (−0.8769, −0.3851)	0.2935 (0.2013, 0.4305)
	Native state vs axial cut	0.1192 (−0.1688, 0.4110)	1.1399 (0.8374, 1.5601)
	Coil cut vs native state	−21.03 (−28.59, −14.27)	0.06216 (0.03306, 0.1154)
Work of adhesion (μJ)	Coil cut vs axial cut	−14.02 (−22.53, −6.589)	0.09243 (0.04303, 0.1938)
	Native state vs axial cut	7.010 (−4.503, 17.74)	1.486 (0.8147, 2.804)

Difference and ratio values are estimates and 95% highest density interval (HDI). Bold indicates a significant difference according to the 95% HDI, indicating a ratio that lies completely outside a range of 0.8 to 1.25.

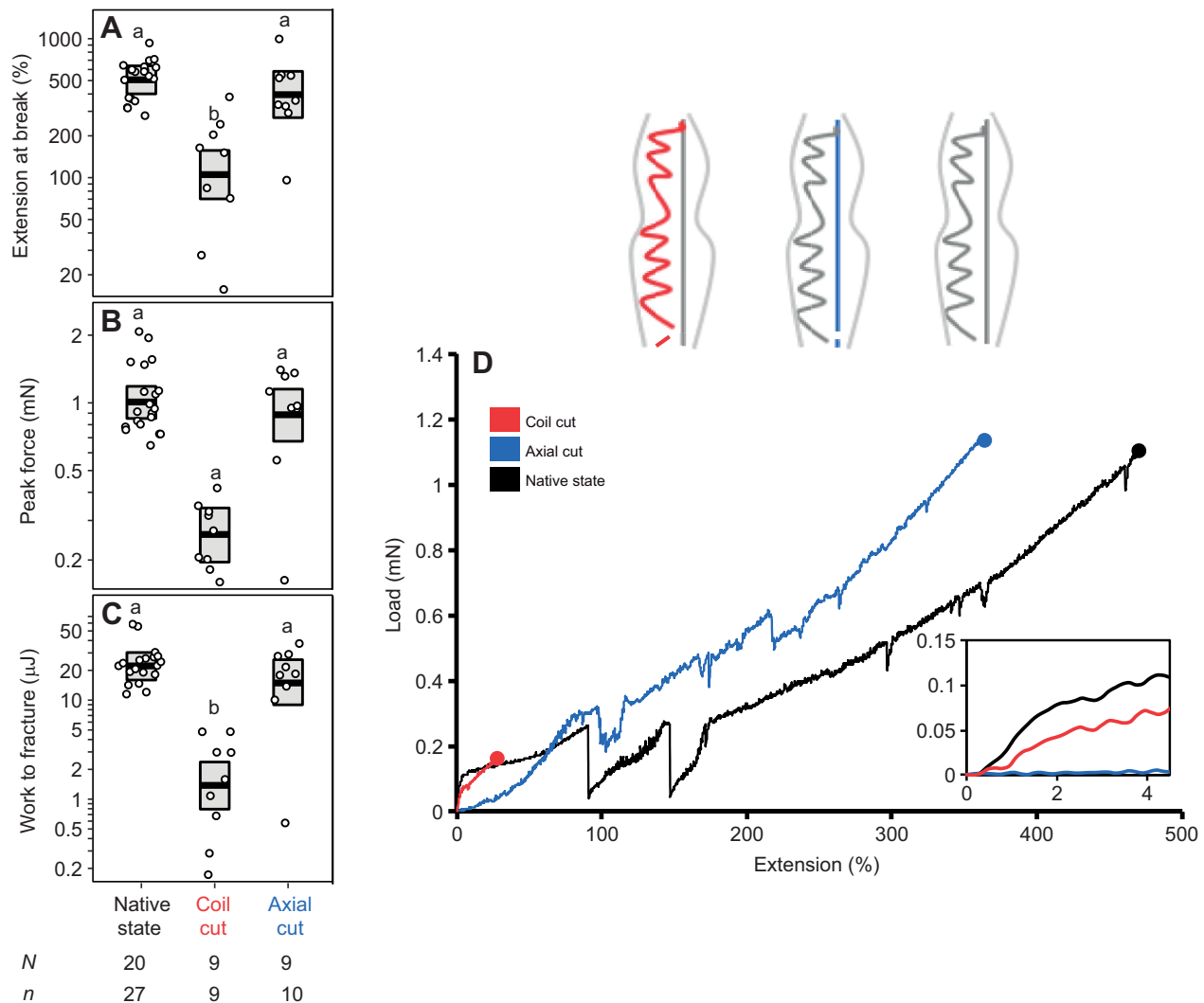


Fig. 5. Tensile properties of *P. clavus* cribellate silk threads in different states. (A) Native state, (B) with a cut coiled fiber (coil cut) and (C) with a cut axial fiber (axial cut). Bars indicate the posterior means \pm 95% highest posterior density intervals from a general linear mixed-effect model. Open circles indicate the average values per spider. Lowercase letters above bars indicate significant differences from the results of pairwise *post hoc* comparisons among thread types. *N* and *n* denote the sample size of spiders and threads, respectively. (D) Representative load–extension curves. Filled circles at the end of the load–extension curves indicate entire thread failure. Inset, close-up of initial mechanical behavior of cribellate threads.

DISCUSSION

Mechanical behavior of cribellate threads with a coiled fiber

Cribellate silk produced by the web-building spider *P. clavus* is a composite biomaterial composed of two constituent silk fibers, i.e. an axial fiber and a coiled fiber, and a surrounding mass of adhesive cribellate nanofibrils. Visualization of cribellate silk during stretching paired with tensile testing of native-state and manipulated threads allowed us to observe novel characteristics of each constituent fiber. First, we found that axial fibers can perform work even after breakage (Movie 1) at least until full tensile engagement of the coiled fiber or potentially even throughout

elongation (Fig. 4A). Second, we found that the coiled fiber greatly improves the work to fracture of the entire thread by imparting increased extensibility and peak load (Fig. 5A–C).

Previous studies by Blackledge and Hayashi (2006a) used cribellate silk from orb web species *Hyptiotes cavatus*, *Hyptiotes gertschi* and *Uloborus diversus*, all Uloboridae whose derived capture threads have lost the coiled fibers and only include cribellate nanofibrils, paracribellate fibers and a pair of axial fibers. Blackledge and Hayashi (2006a) found that the axial fiber broke only once after reaching peak load at \sim 50% extension followed by an additional \sim 100% extension by the cribellate nanofibrils

Table 2. Results of multiple comparisons of adhesive properties to bee thorax and smooth surface

Dependent variable	Difference	Ratio
Extension at detachment (mm mm^{-1})	0.9030 (0.1044, 1.968)	8.056 (2.607, 25.84)
Peak force (mN mm^{-1})	0.0409 (–0.00179, 0.0409)	4.836 (1.3765, 17.4606)
Work of adhesion (μJ)	0.2828 (–0.006795, 0.7586)	32.97 (2.686, 487.2)

Difference and ratio values are estimates and 95% highest density interval (HDI). Bold indicates a significant difference according to the 95% HDI, indicating a ratio that lies completely outside a range of 0.8 to 1.25.

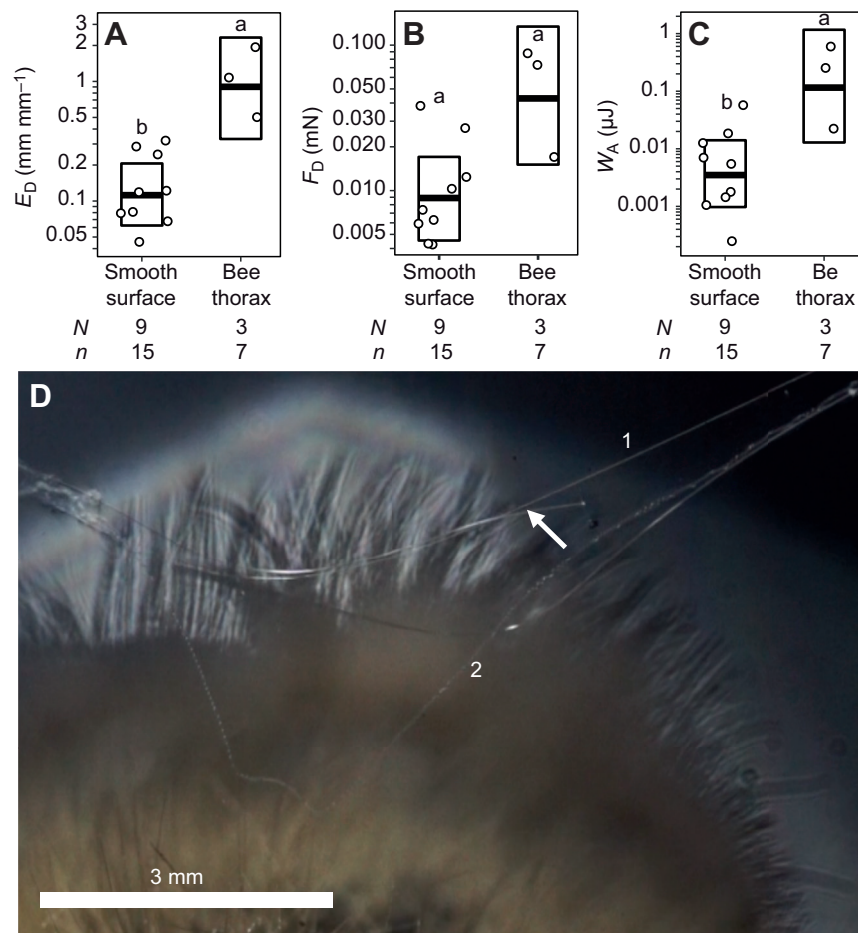


Fig. 6. Adhesive performance of *P. clavus* cribellate silk threads. (A–C) Comparison of extension at detachment (E_D ; A), force at detachment (F_D ; B) and work of adhesion (W_A ; C) of cribellate silk threads when horizontally oriented and pressed into a smooth surface (silicon wafer) or hairy bee thorax (*Apis mellifera*). Bars indicate the posterior mean \pm 95% highest posterior density interval from a general linear mixed-effect model. Open circles indicate the average performance per spider. Lowercase letters above bars indicate significant differences from results of pairwise *post hoc* comparisons among surface types. N and n denote the sample size of spiders and threads, respectively. (D) Image of a cribellate silk thread adhering to a hairy bee thorax. Numbers indicate the constituents of a cribellate silk thread: (1) axial fiber, (2) coiled fiber. Pieces of web frame silk threads (white arrow) can also be seen attached to the cribellate silk thread but are not involved during adhesion.

generating ~25% the maximum load of the axial threads. However, Blackledge and Hayashi (2006a) also observed that silk from *Deinopis spinosa* was very different and could stretch to ~500% original length, similar to results we obtained for *P. clavus* (Fig. 5). Blackledge and Hayashi (2006a) indicated that 92% of the work performed by the entire thread was performed post-axial break and speculated that some of the increase in load could be accounted for through deformation of the coiled fiber, which our investigation supports with clear, empirical data.

Tensile testing of native-state and manipulated cribellate threads of *P. clavus* coupled with visual evidence (Figs 4, 5) allowed us to develop a basic model for how each constituent fiber type contributes to mechanical performance. Early work performed by the cribellate thread, i.e. the first obvious break of the axial fiber, is likely ascribable to tensile deformation of the axial fiber. This is based on two observations: (1) the coiled fiber still showed a coiled morphology, indicating that deformation is only acting upon the fiber's shear modulus, inducing structural changes, rather than the much stiffer tensile modulus and generating material elongation (Fig. 4B), (2) there was very little contribution by the cribellate nanofibrils, as indicated by cribellate threads failing along with the first break of the axial fiber when the coiled fiber was experimentally cut (Fig. 5D).

The axial fiber continues to perform work beyond its initial break as we observed multiple breaks of the axial fiber with corresponding peaks and drops in load on the cribellate thread (Fig. 4). Because loading on the entire thread is not reduced to zero following any break of the axial fiber, forces must be transferred to

the coiled fiber and cribellate nanofibrils, in some, presently unknown, ratio. The exact point at which these constituents are engaged is also unknown. However, as the axial fiber can break an additional 1–2 times, the load that is regenerated typically does not surpass, or only slightly surpasses, the load generated at the initial axial rupture, indicating that work contributions by the cribellate nanofibrils and coiled fiber remain stagnant during this period.

It is not until the coiled fiber becomes fully taut and begins tensile elongation, which corresponds to an inflection point in the force–extension curve, that there is a gradual increase in load beyond what can be achieved by the axial fiber alone (~0.25 mN; Fig. 4). The remaining work done by the thread until failure can likely be primarily attributed to the tensile elongation of the coiled fiber (Figs 4, 5). Cribellate fibrils that did not fail along with the coiled fibers could only generate up to 0.1 mN of tensile load, similar to those of *Uloborus* and *Hyptiotes* (Blackledge and Hayashi, 2006a). We do not know the extent of axial fiber work contribution during this period of deformation because of the difficulty in identifying axial breaks, as extension causes increased proximity of the coiled and axial fiber, obstructing visibility. Nonetheless, the total expected combined loading of the cribellate nanofibrils and axial fiber would be ~0.35 mN, which is less than 50% of the loading at complete thread failure at ~1.0 mN (Fig. 5B).

The complex interplay of constituent silk fibers we observed allows us to identify apparent roles of each constituent of the *P. clavus* composite cribellate silk. Clearly, the axial and coiled fiber act as reinforcement materials, much like rebar used to provide

tensile reinforcement to the cement matrix or calcium carbonate layers of abalone nacre that help prevent crack growth (Ashby and Cebon, 1993; Mayer and Sarikaya, 2002). The coiled fiber makes a significant contribution to the work performed by the overall thread through extreme extensibility achieved via structural changes (facilitated by the shear modulus) and elongation. The axial fiber, although a less significant contributor, is still important to the initial performance of the thread. Evidence of multiple axial breaks indicates that cribellate nanofibrils act as a binder material, conjoining the reinforcement materials and distributing tensile forces throughout the thread. Therefore, it seems the adhesive properties of cribellate nanofibrils have a dual role in the functionality of cribellate silk by attaching to insect prey substrates as well as to the other constituent silk fibers. Together, the synergistic mechanical roles of the constituents of this unique composite material demonstrate a level of integration not previously known to exist in cribellate silk.

Influence of thread morphology on prey capture

The constituent materials of cribellate silk from uloborid orb web spiders (axial fibers and cribellate nanofibrils) are not believed to operate as an integrated system during adhesion. The nanofibrils are thought to perform all the work of adhesion as the axial fibers are too stiff to contribute and deform minimally (Opell and Hendricks, 2007; Sahni et al., 2011). However, a key characteristic in viscid capture silk is the synergy between adhesive material (glue) and flagelliform silk fiber, where forces can be summed across attachment and transferred to the underlying fiber, allowing 50% of the overall work to be performed by the silk fiber (Opell and Hendricks, 2007; Sahni et al., 2010). This is a product of the high compliance of the flagelliform fiber, which is plasticized by the aqueous glue (Gosline et al., 1984; Vollrath and Edmonds, 1989; Swanson et al., 2007). In other systems, such as spider silk attachment discs and glowworm capture threads (Meyer et al., 2014; Piorkowski et al., 2018a), increasing compliance of the underlying fibers through exposure to water or high humidity improves overall adhesion to a substrate. The morphology of the coiled fiber of cribellate silk threads of *P. clavis* may provide an element of compliance analogous to how water plasticizes the core fiber in other systems.

Shear modulus in many natural and synthetic fibers is often 0.5–1 orders of magnitude less than its elastic modulus; for instance, dragline silk from *Nephila clavipes* was previously found to have a shear modulus of 2.38 GPa compared with its elastic modulus of 12.71 GPa (Ko et al., 2001). Therefore, coiling of a fiber reduces the energy needed to deform the structure by initially creating shear forces, i.e. twisting, rather than tensile forces (Ashby and Cebon, 1993). During adhesion testing, where a horizontally oriented thread is pressed into a substrate, we noticed obvious deformation and uncoiling of the coiled fiber (Fig. 6C) when adhering to the hairy bee substrate. The coiled fiber is also in close proximity to where the nanofibrils make attachments to the substrate. The axial fiber bends marginally during these same tests (Fig. 6C) and demarcates the upper edge of the cribellate thread, clearly demonstrating a greater degree of stiffness compared with the coiled fiber. Based on our observation of multiple axial fiber breaks during tensile deformation, which we ascribe to being evidence for distribution of force via cribellate nanofibrils, we speculate that forces generated during adhesion are transferred to the axial and coiled fiber.

Conventional coil springs return to form after deformation within their elastic limit, making them reusable for storing and releasing

energy (Ashby and Cebon, 1993). While the morphology of the coiled fiber resembles coil springs, our observations agree with those of Eberhard and Pereira (1993), as we did not observe recoiling. The coiled fiber was usually permanently warped, losing its original cylindrical morphology and tangling around itself in loose curls after adhesion testing, even when pressed against silicon wafer surfaces. While we cannot rule out the possibility of reversible coiling occurring, particularly at low extension, it seems that energy storage is an unlikely function of the coiled fiber and that it instead contributes to prey capture by damping energy as it permanently deforms.

We found that the adhesive performance of cribellate silk of *P. clavis* increases with surface structures (smooth wafer versus setae of bee thorax) (Fig. 6). Additionally, we show that when one end of a cribellate silk thread adheres to a bee thorax and the other end is stretched, the thread can maintain adhesion with the substrate for more than 50% its overall extensibility. The high extensibility of these threads exhibited during pull-off could serve to dissipate the kinetic energy of prey. Additionally, this extensibility could also expose additional cribellate nanofibrils to the substrate that may form new attachment points rather than only at contact edges as in uloborid cribellate threads, which lack coiled fibers (Hawthorn and Opell, 2003; Opell and Schwend, 2009). *Psechrus clavis* builds horizontal sheet webs, much like other species of cribellate spiders, and typically targets insects that fly or fall into the web. Not all cribellate spiders that produce horizontal webs use capture threads with coiled fibers, e.g. *Hickmania troglodytes* (Austrochilidae), the Tasmanian cave spider (Eberhard and Pereira, 1993; Griswold et al., 2005). However, *P. clavis* may use the high extensibility of their cribellate threads coupled with the force of gravity to cause prey to ‘sink’ into their webs – reducing the insect’s ability to climb or fly up and out of the web.

The high extensibility conferred to cribellate threads by coiled fibers is not available to all cribellate spiders as coiled fibers are totally lacking in all members of one family (Uloboridae), two genera (*Hickmania* and *Matachia*) and some members of another family (Dictynidae) (Griswold et al., 2005). These lineages are very distant from one another, which indicates multiple independent losses of the coiled fiber (Eberhard and Pereira, 1993; Griswold et al., 2005). Another commonality shared amongst these lineages and lacking in all others is that the lateral edges of the cribellate bundle are arranged into regular ‘puffs’ rather than being uniform (Griswold et al., 2005). The puffed morphology observed in these species would likely increase surface area of the thread and the possible number of attachment points that can be made to a substrate (Opell, 1995). These puffs may serve to compensate for the lack of a coiled fiber. Several other factors may also be at play for each lineage. The coiled fiber may have been lost as a result of high metabolic costs involved in production coupled with prey capture not necessitating its presence. For instance, *Hyptiotes* spiders (Uloboridae) employ power amplification to rapidly collapse their spring-loaded triangular webs to entrap prey (Han et al., 2019), a strategy that may not need the high extensibility of individual cribellate threads. Additionally, high extensibility could have been disadvantageous for prey capture in certain instances. Webs with a low density of cribellate silk threads and/or longer individual thread segments may not have benefited from highly extensible threads as prey may have more easily escaped rather than becoming further entwined into the web. Nonetheless, the loss of a coiled fiber is rare among cribellate spiders, with the majority of extant cribellate spiders producing a coiled fiber (Eberhard and Pereira, 1993; Griswold et al., 2005), presumably indicating high functional value.

Conclusions

Psechrus clavis produces cribellate capture threads that are a composite of a pseudoflagelliform axial fiber, a coiled fiber and surrounding cribellate nanofibrils. We found that the composite structure of cribellate silk provides extensibility well beyond that of its individual constituent fibers – the axial fiber breaks early in tensile deformation and multiple times, the coiled fiber gradually unravels and then elongates to increase thread extension by ~6 fold, and the cribellate nanofibrils act as a binder material that supports the reinforcers (axial and coiled fibers) and disperses tensile forces throughout the fibers. Similar to other composite silk systems, gluey spider and glowworm capture silks (Gosline et al., 1984; Vollrath and Edmonds, 1989; Piorkowski et al., 2018b), each component plays a functional role during prey capture. Beyond the established roles of cribellate nanofibrils as the adhesive and the axial fiber as the support, the coiled fiber allows high deformation that maintains attachment during substrate adhesion.

Acknowledgements

We thank Sean D. Kelly for assistance during field collections, and Angela Alicea-Serrano and Sarah Han for assistance with photography and videography.

Competing interests

The authors declare no competing or financial interests.

Author contributions

Conceptualization: D.P., I.-M.T.; Methodology: D.P., T.A.B., A.-C.J., C.-L.W.; Formal analysis: D.P., C.-P.L.; Investigation: D.P., A.-C.J.; Resources: M.W.; Writing - original draft: D.P.; Writing - review & editing: T.A.B., C.-P.L., M.W., I.-M.T.; Visualization: D.P., A.-C.J., M.W.; Supervision: T.A.B., I.-M.T.

Funding

This research was funded by Ministry of Science and Technology, Taiwan grants (MOST 103-2621-B-029-002-MY3; MOST 106-2311-B-029-003-MY3) to I.-M.T., the National Science Foundation to T.A.B., the Deutsche Forschungsgemeinschaft (JO 1464/2-1 to A.-C.J.), Rheinisch-Westfälische Technische Hochschule Aachen (RFwN program to M.W.), and the Excellence Initiative of the German federal and state governments.

Supplementary information

Supplementary information available online at <http://jeb.biologists.org/lookup/doi/10.1242/jeb.215269.supplemental>

References

- Ashby, M. F. and Cebon, D. (1993). Materials selection in mechanical design. *J. Phys.* **IV 3**, C7-1-C7-9. doi:10.1051/jp4:1993701
- Bayer, S. (2012). The lace-sheet-weavers—a long story (Araneae: Psechridae: *Psechrus*). *Zootaxa* **3379**, 1-170. doi:10.11646/zootaxa.3379.1.1
- Blackledge, T. A. and Hayashi, C. Y. (2006a). Unraveling the mechanical properties of composite silk threads spun by cribellate orb-weaving spiders. *J. Exp. Biol.* **209**, 3131-3140. doi:10.1242/jeb.02327
- Blackledge, T. A. and Hayashi, C. Y. (2006b). Silken toolkits: biomechanics of silk fibers spun by the orb web spider *Argiope argentata* (Fabricius, 1775). *J. Exp. Biol.* **209**, 2452-2461. doi:10.1242/jeb.02275
- Blackledge, T. A., Cardullo, R. A. and Hayashi, C. Y. (2005). Polarized light microscopy, variability in spider silk diameters, and the mechanical characterization of spider silk. *Invertebr. Biol.* **124**, 165-173. doi:10.1111/j.1744-7410.2005.00016.x
- Blackledge, T. A., Scharff, N., Coddington, J. A., Szüts, T., Wenzel, J. W., Hayashi, C. Y. and Agnarsson, I. (2009). Reconstructing web evolution and spider diversification in the molecular era. *Proc. Natl. Acad. Sci. USA* **106**, 5229-5234. doi:10.1073/pnas.0901377106
- Blackledge, T. A., Kuntner, M. and Agnarsson, I. (2011). The form and function of spider orb webs: evolution from silk to ecosystems. *Adv. Insect Physiol.* **41**, 175-262. doi:10.1016/B978-0-12-415919-8.00004-5
- Bott, R. A., Baumgartner, W., Bräunig, P., Menzel, F. and Joel, A.-C. (2017). Adhesion enhancement of cribellate capture threads by epicuticular waxes of the insect prey sheds new light on spider web evolution. *Proc. R. Soc. B* **284**, 20170363. doi:10.1098/rspb.2017.0363
- Bürkner, P.-C. (2017). brms: an R package for Bayesian multilevel models using Stan. *J. Stat. Softw.* **80**, 1-28. doi:10.18637/jss.v080.i01
- Cantwell, W. J. and Morton, J. (1991). The impact resistance of composite materials—a review. *Composites* **22**, 347-362. doi:10.1016/0010-4361(91)90549-V
- Eberhard, W. G. (1988). Combing and sticky silk attachment behaviour by cribellate spiders and its taxonomic implications. *Bull. Br. Arachnol. Soc.* **7**, 247-251.
- Eberhard, W. and Pereira, F. (1993). Ultrastructure of cribellate silk of nine species in eight families and possible taxonomic implications (Araneae: Amaurobiidae, Deinopidae, Desidae, Dictynidae, Filistatidae, Hypochilidae, Stiphidiidae, Tengellidae). *J. Arachnol.* **21**, 161-174.
- Elhajjar, R., La Saponara, V. and Muliana, A. (2013). *Smart Composites: Mechanics and Design*. Boca Raton, USA: CRC Press.
- Foelix, R. (2011). *Biology of Spiders*. New York, USA: Oxford University Press.
- Garrison, N. L., Rodriguez, J., Agnarsson, I., Coddington, J. A., Griswold, C. E., Hamilton, C. A., Hedin, M., Kocot, K. M., Ledford, J. M. and Bond, J. E. (2016). Spider phylogenomics: untangling the Spider Tree of Life. *PeerJ* **4**, e1719. doi:10.7717/peerj.1719
- Gosline, J. M., Denny, M. W. and DeMont, M. E. (1984). Spider silk as rubber. *Nature* **309**, 551-552. doi:10.1038/309551a0
- Grannemann, C. C. F., Meyer, M., Reinhardt, M., Ramirez, M. J., Herberstein, M. E. and Joel, A.-C. (2019). Small behavioral adaptations enable more effective prey capture by producing 3D-structured spider threads. *Sci. Rep.* **9**, 17273. doi:10.1038/s41598-019-53764-4
- Griswold, C. E., Coddington, J. A., Platnick, N. I. and Forster, R. R. (1999). Towards a phylogeny of entelegyne spiders (Araneae, Araneomorphae, Entelegynae). *J. Arachnol.* **27**, 53-63.
- Griswold, C. E., Ramirez, M. J., Coddington, J. A. and Platnick, N. I. (2005). Atlas of phylogenetic data for entelegyne spiders (Araneae: Araneomorphae: Entelegynae) with comments on their phylogeny. *Proc. Calif. Acad. Sci.* **56**, 1-324.
- Han, S. I., Astley, H. C., Maksuta, D. D. and Blackledge, T. A. (2019). External power amplification drives prey capture in a spider web. *Proc. Natl. Acad. Sci. USA* **116**, 12060-12065. doi:10.1073/pnas.1821419116
- Hawthorn, A. C. and Opell, B. D. (2003). van der Waals and hygroscopic forces of adhesion generated by spider capture threads. *J. Exp. Biol.* **206**, 3905-3911. doi:10.1242/jeb.00618
- Joel, A.-C. and Baumgartner, W. (2017). Nanofibre production in spiders without electric charge. *J. Exp. Biol.* **220**, 2243-2249. doi:10.1242/jeb.157594
- Joel, A.-C., Kappel, P., Adamova, H., Baumgartner, W. and Scholz, I. (2015). Cribellate thread production in spiders: complex processing of nano-fibres into a functional capture thread. *Arthropod. Struct. Dev.* **44**, 568-573. doi:10.1016/j.asd.2015.07.003
- Jones, R. M. (2014). *Mechanics of Composite Materials*. Boca Raton, USA: CRC press.
- Ko, F. K., Kawabata, S., Inoue, M., Niwa, M., Fossey, S. and Song, J. W. (2001). Engineering properties of spider silk. *MRS Proceedings* **702**, U1.4.1. doi:10.1557/PROC-702-U1.4.1
- Koebly, S. R., Vollrath, F. and Schniepp, H. C. (2017). Toughness-enhancing metastructure in the recluse spider's looped ribbon silk. *Mater. Horiz.* **4**, 377-382. doi:10.1039/C6MH00473C
- Köhler, T. and Vollrath, F. (1995). Thread biomechanics in the two orb-weaving spiders *Araneus diadematus* (Araneae, Araneidae) and *Uloborus walckenaerius* (Araneae, Uloboridae). *J. Exp. Zool.* **271**, 1-17. doi:10.1002/jez.1402710102
- Kovoor, J. (1987). Comparative structure and histochemistry of silk-producing organs in arachnids. In *Ecophysiology of Spiders* (ed. W. Nentwig), pp. 160-186. Berlin: Springer.
- Kullmann, E. (1975). Die Produktion und Funktion von Spinnenfäden und Spinnengewebe. In *Netze in Natur und Technik* (ed. F. Otto), pp. 318-378. Stuttgart, Germany: Institut für leichte Flächentragwerke (IL).
- Lai, C.-W., Zhang, S., Piorkowski, D., Liao, C.-P. and Tso, I.-M. (2017). A trap and a lure: dual function of a nocturnal animal construction. *Anim. Behav.* **130**, 159-164. doi:10.1016/j.anbehav.2017.06.016
- Mayer, G. and Sarikaya, M. (2002). Rigid biological composite materials: structural examples for biomimetic design. *Exp. Mech.* **42**, 395-403. doi:10.1007/BF02412144
- Meyer, A., Pugno, N. M. and Cranford, S. W. (2014). Compliant threads maximize spider silk connection strength and toughness. *J. R. Soc. Interface* **11**, 20140561. doi:10.1098/rsif.2014.0561
- Michalik, P., Piorkowski, D., Blackledge, T. A. and Ramirez, M. J. (2019). Functional trade-offs in cribellate silk mediated by spinning behavior. *Sci. Rep.* **9**, 9092. doi:10.1038/s41598-019-45552-x
- Opell, B. D. (1995). Ontogenetic changes in cribellum spigot number and cribellar prey capture thread stickiness in the spider family Uloboridae. *J. Morphol.* **224**, 47-56. doi:10.1002/jmor.1052240106
- Opell, B. D. and Hendricks, M. L. (2007). Adhesive recruitment by the viscous capture threads of araneoid orb-weaving spiders. *J. Exp. Biol.* **210**, 553-560. doi:10.1242/jeb.02682
- Opell, B. D. and Schwend, H. S. (2009). Adhesive efficiency of spider prey capture threads. *Zoology* **112**, 16-26. doi:10.1016/j.zool.2008.04.002
- Patek, S. N., Korff, W. L. and Caldwell, R. L. (2004). Biomechanics: deadly strike mechanism of a mantis shrimp. *Nature* **428**, 819. doi:10.1038/428819a
- Peters, H. M. (1984). The spinning apparatus of Uloboridae in relation to the structure and construction of capture threads (Arachnida, Araneida). *Zoomorphology* **104**, 96-104. doi:10.1007/BF00312023

- Peters, H. M.** (1992a). Über Struktur und Herstellung von Fangfäden cribellater Spinnen der Familie Eresidae (Arachnida, Araneae). *Verh. Naturwiss. Ver. Hamburg* **33**, 213-227.
- Peters, H. M.** (1992b). On the spinning apparatus and the structure of the capture threads of *Deinopis subrufus* (Araneae, Deinopidae). *Zoomorphology* **112**, 27-37. doi:10.1007/BF01632992
- Piorkowski, D. and Blackledge, T. A.** (2017). Punctuated evolution of viscid silk in spider orb webs supported by mechanical behavior of wet cribellate silk. *Sci. Nat.* **104**, 67. doi:10.1007/s00114-017-1489-x
- Piorkowski, D., Blackledge, T. A., Liao, C.-P., Doran, N. E., Wu, C.-L., Blamires, S. J. and Tso, I.-M.** (2018a). Humidity-dependent mechanical and adhesive properties of *Arachnocampa tasmaniensis* capture threads. *J. Zool.* **305**, 256-266. doi:10.1111/jzo.12562
- Piorkowski, D., Blamires, S. J., Doran, N. E., Liao, C.-P., Wu, C.-L. and Tso, I.-M.** (2018b). Ontogenetic shift toward stronger, tougher silk of a web-building, cave-dwelling spider. *J. Zool.* **304**, 81-89. doi:10.1111/jzo.12507
- Popescu, C. and Höcker, H.** (2007). Hair—the most sophisticated biological composite material. *Chem. Soc. Rev.* **36**, 1282-1291. doi:10.1039/b604537p
- Roberts, T. J. and Azizi, E.** (2011). Flexible mechanisms: the diverse roles of biological springs in vertebrate movement. *J. Exp. Biol.* **214**, 353-361. doi:10.1242/jeb.038588
- Sahni, V., Blackledge, T. A. and Dhinojwala, A.** (2010). Viscoelastic solids explain spider web stickiness. *Nat. Commun.* **1**, 19. doi:10.1038/ncomms1019
- Sahni, V., Blackledge, T. A. and Dhinojwala, A.** (2011). A review on spider silk adhesion. *J. Adhes.* **87**, 595-614. doi:10.1080/00218464.2011.583588
- Swanson, B. O., Blackledge, T. A. and Hayashi, C. Y.** (2007). Spider capture silk: performance implications of variation in an exceptional biomaterial. *J. Exp. Zool. A Ecol. Genet. Physiol.* **307A**, 654-666. doi:10.1002/jez.420
- Vollrath, F. and Edmonds, D. T.** (1989). Modulation of the mechanical properties of spider silk by coating with water. *Nature* **340**, 305-307. doi:10.1038/340305a0
- Zschokke, S. and Vollrath, F.** (1995). Unfreezing the behaviour of two orb spiders. *Physiol. Behav.* **58**, 1167-1173. doi:10.1016/0031-9384(95)02062-4